REVIEW ARTICLE

Current status of the application of additive-manufactured TPMS structure in bone tissue engineering

Yosef Wakjira[1] · Arturo Cioni[2] · Hirpa G. Lemu[1]

Abstract

Bone tissue engineering provided the innovative solution to regenerate bone tissue using scaffolds (porous) structures. This research investigates optimization, additive manufacturing methods and the application areas of triply periodic minimal surface-based (TPMS) porous structures in the broad field of tissue engineering through literature review. The properties of TPMS structures are compared with more classical strut-based structures. Also, information on how TPMS can be formulated and how they can be designed to obtain desired properties are presented. Attention is dedicated to the topological optimization process and how it can be applied to scaffolds to further increase their biomechanical properties and improve their design through density, heterogenization, and unit cell size grading. Common numerical algorithms as well as the difference between gradient-based and non-gradient-based algorithms are proposed. Efforts also include the description of the main additive manufacturing technologies that can be utilized to manufacture either stochastic or periodic scaffolds. The information present in this work should be able to introduce the reader to the use of TPMS structures in tissue engineering.

Keywords TPMS · Tissue engineering · Scaffolds · Additive manufacturing

Abbreviations

AM	Additive manufacturing
BCC	Body centered cubic
BCP	Biphasic calcium phosphate
BESO	Bidirectional evolutionary structural optimization
BTE	Bone tissue engineering
CAD	Computer-aided design
CHA	Carbonated hydroxyapatite
CFD	Computational fluid dynamics
CT	Computer tomography
DLP	Digital light processing
EBM	Electron beam melting
FCC	Face-centered cubic
FDM	Fused deposition modeling
FEM	Finite elements method
FFF	Fused filament fabrication
GB	Gradient-based
IWP	I-wrapped-package
LS	Level set method
MMC	Moving morphable components
NGB	Non-gradient-based
nTO	Nano-topological optimization
PCL	Polycaprolactone
RAI	Root analog implant
RD	Relative density
SEM	Scanning electron microscope
SIMP	Solid isotropic material with penalization
SLA	Stereo-lithography apparatus
SLS	Selective laser sintering
TBM	Total bone marrow
TPMS	Triply periodical minimal surfaces
TO	Topological optimization
UV	Ultraviolet

✉ Yosef Wakjira
yosef.w.adugna@uis.no

1 Faculty of Science and Technology, Department of Mechanical and Structural Engineering and Materials Science, University of Stavanger, Kjell Arholms Gate 41, 4021 Stavanger, Norway

2 Scuola di Ingegneria, Dipartimento di Ingegneria Industriale, Università degli Studi di Firenze, Via di S. Marta 3, 50139 Florence, Italy

1 Introduction

In recent years, there has been a lot of interest in developing a better alternative to classic bone lesion repair techniques such as bone autografts or allografts. The former has

the chance of causing morbidity of the donor site, which is pain, inflammation, and other complications, while the latter requires a compatible donor and there is a risk of disease transmission [1, 2]. The medical industry has been using prostheses to replace big bone sections. These parts are expensive since they require a choice of biocompatible material and a lot of process time to achieve adequate geometrical accuracy and surface quality, especially since standard manufacturing techniques are employed [3, 4]. A further improvement for bone implants, which is cheaper, more customizable, and not limited to big replacements is scaffolds.

Scaffolds are porous structures, also called lattices, developed to aid bone regeneration by promoting cellular adhesion, proliferation, and differentiation. If properly designed, new bone tissue develops inside the scaffold itself, achieving osteointegration, the acceptance of live bone tissue of the implant, and eventually bone repair. Lattices can be differentiated into two main families: strut-based or surface-based [5]. Strut-based lattices are better known and are composed by repeating units made of intersecting beams called struts [6]. These kinds of scaffolds are controllable only by adjusting length and radius of the cell's struts which is limiting in terms of properties manipulation. Furthermore, the connections between cells are not smooth and lead to stress concentration which is not desirable [7].

While the structures built with classic methods have been researched for their useful characteristics, the most recent frontier explores surfaced-based structures made of unit cells derived from triply periodic minimal surface (TPMS).

TPMSs have first been described by Schwarz in 1865 [8]. They exhibit peculiar properties as they result periodic in three dimensions, non-self-intersecting, easily defined by a parametric equation and exhibit zero mean curvature at every point [7, 9–12]. As research continued, more and more different types of TPMS got proposed with numbers now in the hundreds although only a limited amount are of interest for engineering purposes mostly due to their simple definition, manufacturability, or mechanical properties [13, 14].

The parametric formulation of TPMSs makes surface features easily manipulable for many fields. High volume or mass-specific qualities like surface, stiffness, and yield strength are preferred in mathematical entities since they are beneficial in many fields [15, 16]. Sengsri et al. [15] used Schwarz basic geometry to model and build a bridge-bearing scaffold for civil engineering. Ouda et al. [17] used lattice design for static mixers to compare energy requirements and efficiency against classic designs and found that TPMSs improve water treatment facility performance. Qureshi et al. [9] compared gyroid, primitive, and I-Wrapped Package (IWP) cells to Kelvin cell strut-based structures in latent heat thermal energy storage systems and found that TPMS-based design performs better. Peng et al. [11] streamlined TPMS-based heat exchanger design with a design procedure.

In mechanical engineering, Al-Ketan et al. [18] proposed a catalytic substrate with few surfaces that has remarkable mechanical and fluid dynamics features including low lattice pressure drops. To achieve higher hydrogen storage density and transfer rate, Lesmana et al. [19] used metal hydrides in a TPMS-based structure which was also lightweight compared to traditional designs. Yang et al. [20] proposed a design to acoustically isolate sound in the upper midrange frequency range which were easily through the parametric design. In nuclear engineering, improved fuel rods design based on TPMSs have been proposed by Martin et al. [21].

Due to their high surface-to-volume ratio, good mechanical qualities, lightweight structure, and smooth surfaces that facilitate fluid interactions, TPMS are prominent in engineering. Biomedical uses include dental and bone tissue engineering [22–24], chemical use for catalytic substrates to hydrogen storage [18, 19], civil (construction) applications for structural and hydraulic [15, 17], mechanical applications for acoustic, energy, and thermal [9, 11, 20], and nuclear applications for fuel rods [21]. Figure 1 outlines several engineering uses of TPMSs from this study's literature review.

For biomedical applications, TPMSs are praised for their permeability, that is allowing mass flow without excessive drop in pressure [18, 23–25], which is directly linked with successful cell adhesion and proliferation [23–27]. Also important is the possibility of altering the relative density of the scaffold to closely resemble the elasticity modulus of live bone tissue to avoid the issue known as stress shielding which causes the bone close to the implant to weaken [2, 5, 10, 16, 26–28]. The most important scaffolds properties can be summarized in mechanical strength, chemical stability, and biological compatibility [29]. The porous structure inside live bone is not uniform, but its density changes as a function of space. While uniform lattices have been designed and successfully manufactured as scaffolds, they are not able to replicate the transition zone between cortical and trabecular bone [5]. In this case, more complicated structures are required known as functionally graded scaffolds whose relative density is continuously altered along one or more principal directions [16, 30]. Further optimization of density can be achieved through a process of topological optimization. In recent years, the development of AM allows scaffolds to be realized in a relatively cheap manner thanks to the "complexity for free" and "batch size independence" of this technology [16].

The aim of this article is to explore reported works on TPMS optimization techniques, their manufacturing technique through additive manufacturing technology and their application in a wide range of different medical field. Different TPMS geometries including mathematical representations and design options, functional grading strategies, related commonly utilized algorithms for topology
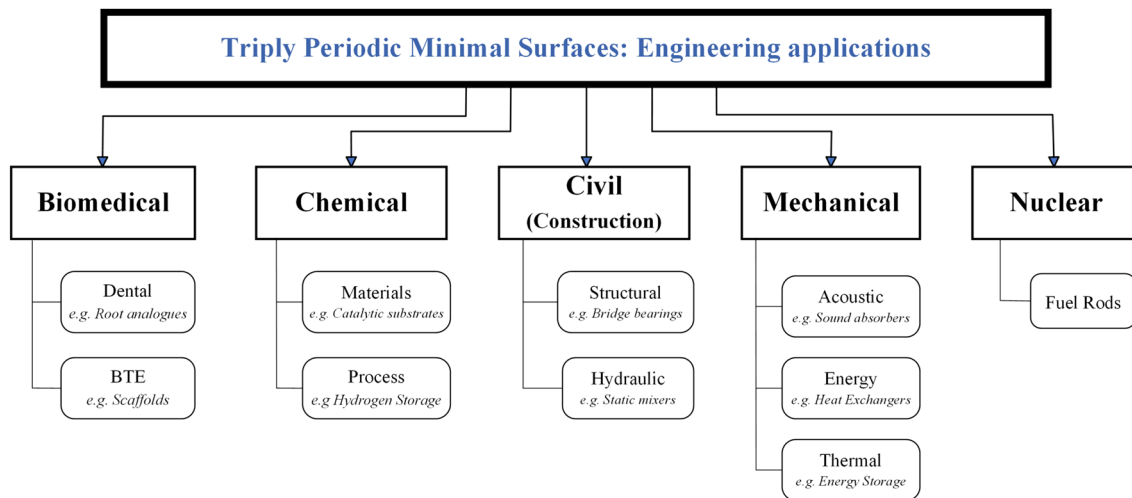
Fig. 1 Summary overview of TPMS applications

optimization and the proper objective functions. The article also describes functional grading strategies and recommends manufacturing techniques suitable for production of TPMS structures.

2 Porous structures and TPMS's

Tissue engineering uses biology, material sciences, medicine, computational simulations, and manufacturing. Human long bones have two primary regions: the cortex, which is denser and stiffer for load-bearing, and the trabecular, which is porous and lightweight for transporting nutrients and waste [2, 5, 26, 27, 31, 32]. The human body is capable of adequately healing bone damage on its own if lesions are smaller than 2 cm [2]. To treat larger injuries, autografts or allografts are used. Standards involve transplanting live bone tissue from the patient or external donors. Generally well understood, they can induce donor discomfort, pain, infection around the grafting site, or material rejection [2, 27, 31, 33].

BTE creates porous structures that can endure stress and allow cells to adhere and disperse for osteointegration and bone regeneration. A scaffold replicates an extracellular matrix for cell growth and differentiation [2, 31, 34]. The most common geometries of strut-based are the BCC [35], the FCC [36], or the Auxetic [37].

TPMSs are mathematically defined implicit surfaces that divide the domain space into 2 non-intersecting regions: if the morphology of the regions is similar it is said the TPMS is balanced, i.e., gyroid, otherwise it is deemed unbalanced, as IWP or Neovious [5, 16]. Their surface is continually smooth, with zero mean curvature since curvatures through main orthogonal planes are equal and opposite [10]. They

can be formulated through Enneper-Weierestrass [38–40] representation using a system of complex equations or as an approximation of a Fourier series, called level set equations [10, 16, 41, 42], which take the form of f (X, Y, Z) = C (X, Y, Z). In this case, $X, Y, Z = 2\pi \frac{n_i}{L_i}$ with n being the number of unit cells and L being cell size in "i" dimension. Some common TPMS formulations in level set form are presented in the following list:

1. *Gyroid*— $f(X, Y, Z) = \sin(X)\cos(Y) + \sin(Y)\cos(Z) + \sin(Z)\cos(X)$
2. *Primitive*— $f(X, Y, Z) = \cos(X) + \cos(Y) + \cos(Z)$
3. *Diamond*— $f(X, Y, Z) = \cos(X)\cos(Y)\cos(Z)$
4. *Nevoius*— $f(X, Y, Z) = 3(\cos(X) + \cos(Y) + \cos(Z) + 4\cos(X)\cos(Y)\cos(Z)$
5. *SplitP*— $f(X, Y, Z) = 1.1(\sin(2X)\cos(Y)\sin(Z) + \sin(2Y)\cos(Z)\sin(X) + \sin(2X)\cos(X)\sin(Y)) - 0.2(\cos(2X)\cos(2Y)\cos(2Z) + \cos(2Z)\cos(2X)) - 0.4(\cos(2Y) + \cos(2Z) + \cos(2X))$
6. *Lidinoid*— $f(X, Y, Z) = 0.5(\sin(2X)\cos(Y)\sin(Z) + \sin(2Y)\cos(Z)\sin(X) + \sin(2Z)\cos(X)\sin(Y)) - 0.5(\cos(2X)\cos(2Y) + \cos(2Y)\cos(2Z) + \cos(2Z)\cos(2X)) + 0.15$

TPMS scaffolds can be realized in two different ways: by offsetting the surface and obtaining a solid "sheet-like" solid component or by solidifying one of the 2 regions created in the design space, creating a "skeleton-like" solid [5, 7]. Sheet structures generally present a stretching deformation mode and better mechanical properties than their skeletal counterparts and their bending deformation mode [7, 10, 43, 44]. Figures 2 and 3 illustrate the contrasting characteristics of Sheet-based and skeletal-based TPMS geometries. These

Fig. 2 Examples of sheet-based TPMS geometries. **a** Gyroid **b** Primitive **c** Diamond **d** Neovius **e** Split P **f** Lidinoid
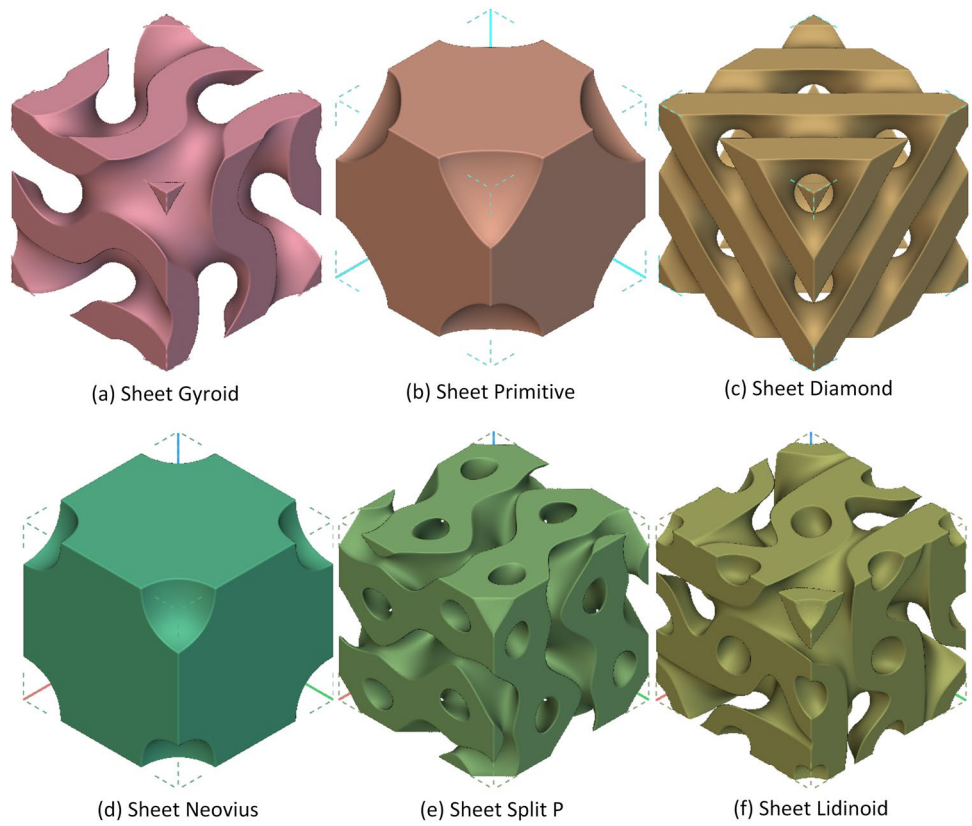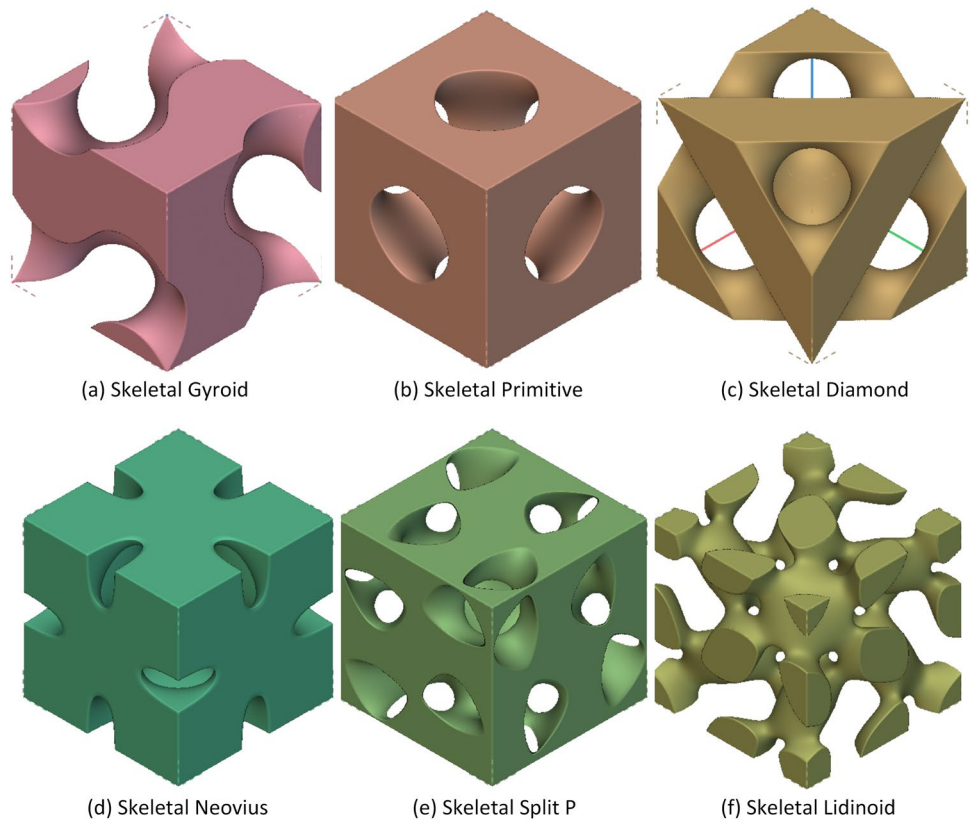
(a) Sheet Gyroid

(b) Sheet Primitive

(c) Sheet Diamond

(d) Sheet Neovius

(e) Sheet Split P

(f) Sheet Lidinoid

Fig. 3 Examples of skeletal-based TPMS geometries. **a** Gyroid **b** Primitive **c** Diamond **d** Neovius **e** Split P **f** Lidinoid

(a) Skeletal Gyroid

(b) Skeletal Primitive

(c) Skeletal Diamond

(d) Skeletal Neovius

(e) Skeletal Split P

(f) Skeletal Lidinoid

figures showcase selected geometries, namely (a) Gyroid, (b) Primitive, (c) Diamond, (d) Neovius, (e) Split P, and (f) Lidinoid.

Scaffolds can also be graded or uniform, depending on whether their unit cell geometry is constant across the design space. $C(X,Y,Z) = 0$ for uniform structures. Grading is a powerful technique for customizing scaffold properties to the researched use case. As shown in Fig. 4, heterogenous grading or hybridization, unit cell size or multi-scale grading, and density-based grading are the main grading methods.

Heterogenous grading (Fig. 4a) involves combining multiple TPMS morphologies to better satisfy scaffold requirements by mixing properties found in different geometries, such as permeability and mechanical strength [16, 30]. The most challenging aspect of this strategy is designing a transition region between TPMSs to assure continuity and avoid stress concentration. Unit cell size grading (Fig. 4b) gradually increases or decreases unit cell dimensions to create a metamaterial closer to a solid than a porous structure in particular scaffold sections [16, 43]. Hierarchical design, to its extreme, incorporates unit cell design at multiple scales of structures with great surface area but precise manufacture [44]. Density-based grading (Fig. 4c) increases or decreases domain wall thickness coherently with the level set constant [16]. The ratio of the porous metamaterial's density to the solid lattice material's density is called relative density. It can also be understood as a volume ratio between the lattice volume and the identical void-less lattice [5].

Additive manufacturing is the most chosen approach for manufacturing BTE scaffolds because it can manufacture complex geometries affordably and has a vast material library and metal, ceramic, and polymer processing processes. As metal processing is primarily powder-based, part quality depends on powder. Selective Laser Sintering (SLS), Selective Laser Melting (SLM), or Electron Beam Melting (EBM) addresses stainless steel and titanium alloys, the most common materials, depending on powder melting temperatures and quality. Ceramics are rarely used for scaffolds. However, some release ions that feed bone minerals [2, 31]. Used as a suspension in UV-sensitive Stereolithography Apparatus (SLA) resins [33, 45], as a reinforcing component in extruded composites, or in powder techniques [31]. Most powder, resin, and extrusion-based 3D printing technologies use polymers, which are easy to print. Biodegradable polymers like Polycaprolactone (PCL) are also popular [2, 31, 46, 47].

3 Applications of TPMS in tissue engineering

The applications of TPMS structures range from neurosurgery to maxillofacial, joint orthopedics to spine surgery, and various orthopedics areas. Some of the in-depth analyses on the application of TPMS in a varying range of medical field are discussed under this section. Figure 5 describes different application areas of TPMS in medical and biomedical field.

3.1 Neurosurgery

Neurosurgery is one of the areas where TPMS structures became impactful. Paré et al. [48] researched healing of craniofacial bone defects. Biphasic calcium phosphate (BCP) and carbonated hydroxyapatite (CHA) scaffolds designed with TPMS topology were tested against classic BCP granules. The in vivo test was carried out with 2 groups, one with scaffolds seeded with total bone marrow cells (TBM) while the other wasn't. The results after 7 weeks showed that bone growth was greater and more homogenous in TPMS-based scaffolds than in the granules-based procedure.

Carluccio et al. [49] SLM manufactured Fe-25Mn alloy-graded scaffold designed with Primitive TPMS at 58% RD. Tests were done on microstructure quality, mech props, and corrosion resistance as well as biological compatibility. The
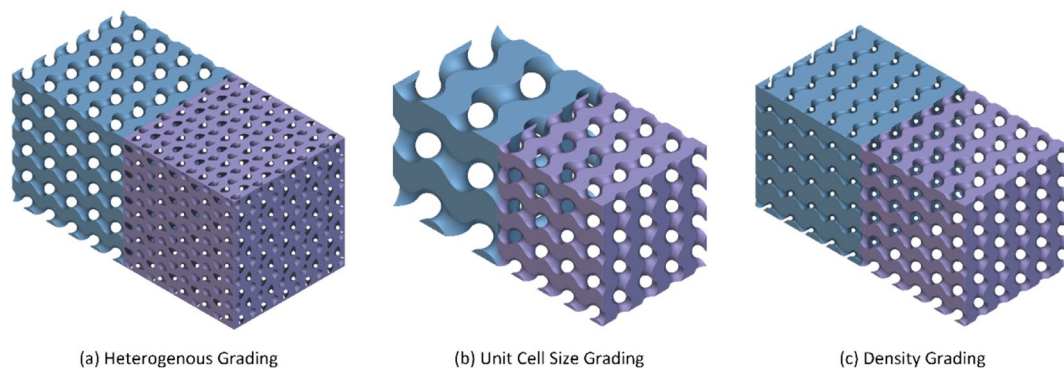

Fig. 4 Three different possible strategies to achieve functional grading in a porous structure. **a** Heterogenous grading **b** Unit cell size grading **c** Density grading
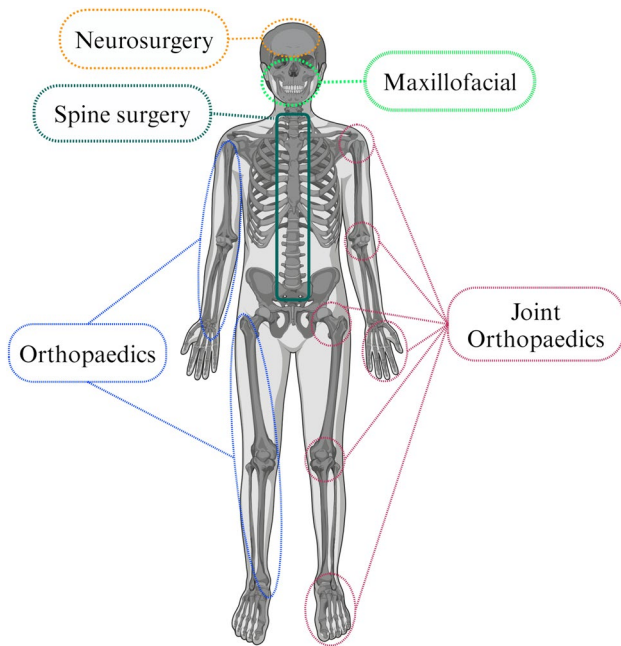
(a) Heterogenous Grading   (b) Unit Cell Size Grading   (c) Density Grading

Fig. 5 Application areas of TPMS in bone tissue engineering

material shows itself to be highly ductile but with mechanical props sufficient for load-bearing applications even after a 28-day period in recreated physiological conditions. Corrosion resistance was inferior when compared to pure iron solid iron. In vitro cell testing showed good biocompatibility with good osteoblast adhesion which prompted an in vivo study. Bone integration on calvarial defect was successful and the results were verified after 4 weeks: from micro-CT scans, it is evident how new bone formation infiltrated into the scaffold completely integrating it into the skull.

3.2 Maxillofacial

The remarkable use of TPMS in maxillofacial has been observed. Zheng et al. [50] proposed a mandible implant modeled using reverse engineering from CT data and Gyroid TPMS geometry, both skeletal- and sheet-based. SLM was used for manufacturing the Ti6Al4V scaffold at 30% RD. Post-processing was required to remove residual stresses, to obtain adequate surface quality and increase available surface: the printed part was first heat treated and then sandblasted, and finally acid etched. The results show a valid alternative to commercially available mandibular implants since TPMS-based scaffolds are easily customizable to the patient's mandibular morphology through reverse engineering techniques and it has better mechanical properties than standard BCC lattices. Song et al. [22] designed a dental root analog implant (RAI) made of Ti6Al4V and designed with P and G TPMS topology. The morphology emulates actual root shape to better fit the cavity, in contrast with

commercial solid implants that are fit in place and the gaps are filled with bone powder. The high porosity, the interconnectivity, and the biocompatibility of the material alleviate stress shielding issues and improve osseointegration in the alveolar bone wall, where the root analog perfectly fits. The FEM analysis result shows promising results, but experiments in an environment like the oral cavity should be performed.

3.3 Joint orthopedics

Different researchers identified the use of TPMS for different joint orthopedics for BTE. Yoo [51] proposed a hierarchical scaffold design method using recursive Boolean operations and TPMSs. Both porosity and pore architecture gradients were controllable and used in the study to design talus bone scaffolds with varying level of porosity, with different pore scales and with hybridization techniques on different scales. This allows create implants that are capable of mimicking bone macrostructure, cortical and trabecular, and microstructure, osteons and trabeculae. Zhu et al. [52] developed primitive and gyroid-based scaffold, with varying RD between 53 and 63%, to reduce stress levels on the joint system caused by meniscal implant. According to FEM simulations, a solid implant causes up to 26.8 MPa and 34.1 MPa which causes deformation of healthy tissue, discomfort and lack of mobility in the patient.

Corona-Castuera et al. [53] manufactured a partial hip implant designed through tomography data and gyroid and double gyroid TPMSs to emulate patient bone density. The metamaterials were tested under uniaxial compression loads to ensure similar mechanical properties to the host's bone, where the simple gyroid performed better than the Double Gyroid sample. The prosthesis was manufactured through SLM with 17-4 PH stainless steel obtaining a very lightweight (72 g) part when compared to solid alternatives. The methodology followed in the paper can be followed to obtain customizable implants with better performances and comfort for the patient, although further cell culturing testing would be required. Koplin et al. [54] made use of AI to design 3D models of a finger joint implant from 2D X-ray images with a porous structure defined by split P unit cells. The model evaluated and then printed with silicon nitride-based ceramics through SLA. The model was mechanically tested via B3B, and compression test and the total implant load was simulated through FEM.

3.4 Long bones orthopedics

Similarly, Verma et al. [55] created a personalized Ti6Al4V scaffold design to heal segmental bone defect of a femur, making use of primitive and gyroid geometries, chosen for their biomorphic and biomimicking characteristics. The

results of FEM analysis showed that the stress shielding effect can be greatly reduced using these porous structures while retaining sufficient load-bearing capabilities for bone lesion repair, this makes TPMS-based scaffolds a valid alternative to commonly performed bone grafts. Germain et al. [56] used FDM technology to manufacture a biodegradable PLA scaffold designed with Gyroid topology at 30% RD. The sample underwent a micro-CT scan to assess print quality and porosity and was tested for degradation rate in physiological conditions. The Gyroid showed to be more durable, lasting 64 weeks until degradation, compared to the strut-based counterpart that only survived 33 weeks. Li et al. [40] designed, printed, simulated, and tested in vivo a primitive-based graded scaffold for segmental bone defect at 50% RD. FEM analysis clearly shows that the lattice allows for better stress distribution and overall material usage when compared to a solid sample.

3.5 Spine surgery

Spinal problems are prevalent and expensive. Standard treatment for pain and stabilizing degraded segments involves spinal fusion implants, which have limitations such implant-bone mechanical disparity and poor dynamic response. Research to improve these aspects was proposed by Du et al. [57] who studied the manufacture of TPMS scaffolds for spinal fusion applications created with pure a PEEK/SiN composite as SiN is very favorable for osseointegration but is too brittle while PEEK has desirable mechanical properties but is hydrophobic which makes for poor bone inclusion performance. Gyroid geometry was chosen at 70% RD and manufactured through FDM making use of a self-supporting design. The scaffold underwent FEM and experimental testing, and cell proliferation was observed in vitro: the results were promising for future spinal BTE applications.

To address stress shielding, Qi et al. [58] proposed a porous spinal fusion cage implant made with Ti64AlV a biocompatible material with a design that promotes bone growth while being able to bear loads. Gyroid and primitive geometries were modeled, simulated, printed, and tested. SEM study of printed parts demonstrated cracking from the spot's energy distribution, thermal gradient, and residual stresses. Although all meet the basic requirements, the TPMS structure with varied pore size is better than the uniform or non-TPMS scaffold.

3.6 Cell growth

It is a fundamental requirement of scaffolds built for biomedical applications to be biocompatible and to promote cell adhesion and ingrowth. Melchels et al. [59] designed and printed a 30% RD gyroid scaffold through SLA using PDLLA resins. The research focused on cell seeding, both static and dynamic, incubation, and culturing of mesenchymal stromal cells (iMSC). The scaffold was tested against a stochastic lattice which is manufacturable through commonly known technologies. The stochastic lattice resulted in higher surface area but had less control over pore size (76 μm standard deviation against 126 μm) and significantly higher tortuosity. This leads to a significantly higher permeability for the Gyroid scaffold (0.519 mm^2 against 0.046 mm^2) which is why after 5 days of culturing there is a notable difference in cell ingrowth between the two models: the gyroid shows cell presence deep inside its geometry while the stochastic lattice only developed an external film. It is of note that after 20 days no living cells are found deep into the porous scaffold, probably due to a lack of nutrient transport: this suggests the necessity of mesoscale pores that help with vascularization on top of the micro-scale pores that allow cell proliferation.

4 Design optimization and additive manufacturing of porous structures

The "conventional" manufacturing methods are used to make components in most sectors including machining, casting, and plastic deformations. Casting and plastic deformation cannot create complex structures like TPMSs because porous shapes have too many undercuts to allow die extraction. Except for perishable dies in lost wax casting, the sacrificial model must be hand-made or additively manufactured. Machining TPMS structures is difficult because they are complex surfaces with considerable tortuosity, which varies with the unit cell [60]. For these reasons, conventional methods are unsuitable for TPMS-based scaffold construction.

Additionally, non-conventional manufacturing techniques, such as electrospinning [34], freeze-drying [61], gas-foaming, and particulate leaching [62], were used for porous structures fabrication. However, it is impossible to control the microstructure's topology which makes them unable to create periodic scaffolds but only stochastic ones. In this regard, AM, a collection of technologies that manufactures 3D structures by slicing them into several 2D layers that are joined together is found to be the most effective technique. It is recommended to design the final product by being aware of the limitations of the specific AM technology that is going to be employed in order to obtain a streamlined manufacturing process. The AM technologies suitable for scaffold manufacturing are discussed below in Sect. 4.2.

4.1 Topology-optimized design of TPMS structures

There are multiple approaches to design optimization of complex structures such as TMPSs which help to improve porosity and permeability or mechanical performance of

the scaffold. Among these, the use of reverse engineering based on computerized tomography (CT) data [34] used to reverse engineer the real-life scanned bone into a digital CAD model which is then either used as a basis to create a customized implant or it is itself rendered as a lattice structure by applying TPMS geometry to the original model [53]. In either case, it is required to extract geometrical information of the bone, such as trabecular mean thickness, bone volume, and number of trabeculae [63]. CT scans can also be used to verify the quality of the manufactured part by comparing the resulting scan to the optimal CAD model [64]. Designs can also be obtained by Voronoi tessellation in three dimensions to obtain bone-like trabecular structures [2] and refined through topological optimization. Figure 6 shows CT scan 3D printed part for defect identification and geometrical feature extraction process from CT scan.

Topological optimization is a technique consisting in optimizing material distribution in the design space under defined constraints, like unit cell volume, and boundary conditions, like external loads, that must also ensure material continuity and manufacturability. In conducting topology optimization, an objective function is chosen, and the method aims at either minimizing or maximizing it through an algorithm of choice, among others some of the most common topology optimization algorithms:

- Solid isotropic material with penalization (SIMP).
- Simulated annealing.
- Bidirectional evolutionary structural optimization (BESO).
- Level set method (LS).

- Nano-topology optimization (nTO).
- Moving morphable components (MMC).

Simplified explanation of the algorithms is described below. SIMP is a common methodology that uses a fictional density as a design variable. For 2 phase materials, this density varies between values of 0 and 1, where 0 identifies void regions and 1 dense region. For multiple phases materials, however, there exist slightly more complicated definitions. In case of a stiffness-oriented optimization, the Young´s modulus is expressed as an artificial density weighted combination of the 2 material's modulus. If the second material is a void, then E is set as 0. A threshold is usually employed to remove elements that exhibit an intermediate density so that a clear distinction between solid and void regions is obtained [16, 42, 66–71].

Simulated annealing is a metaheuristic algorithm that permits a limited acceptance of worse configurations to avoid local minima as a solution. The partial solutions are generated through random perturbations. This method is also suitable for large search spaces whose computational load may be too high with other methods [72, 73], whereas bidirectional evolutionary structural optimization method consists of eliminating elements that bear lower amounts of stress (or other parameters inherent to the objective functions) with the possibility of adding new elements adjacent to those that got eliminated, thus obtaining an optimal material distribution [66, 69, 71, 74]. On the other hand, level set method makes use of level set equations to define material boundaries to avoid intermediate densities in a density-based approach. This also allows the TO to avoid numerical anomalies such as mesh checkerboarding effects [42, 66, 71, 75]. Also,
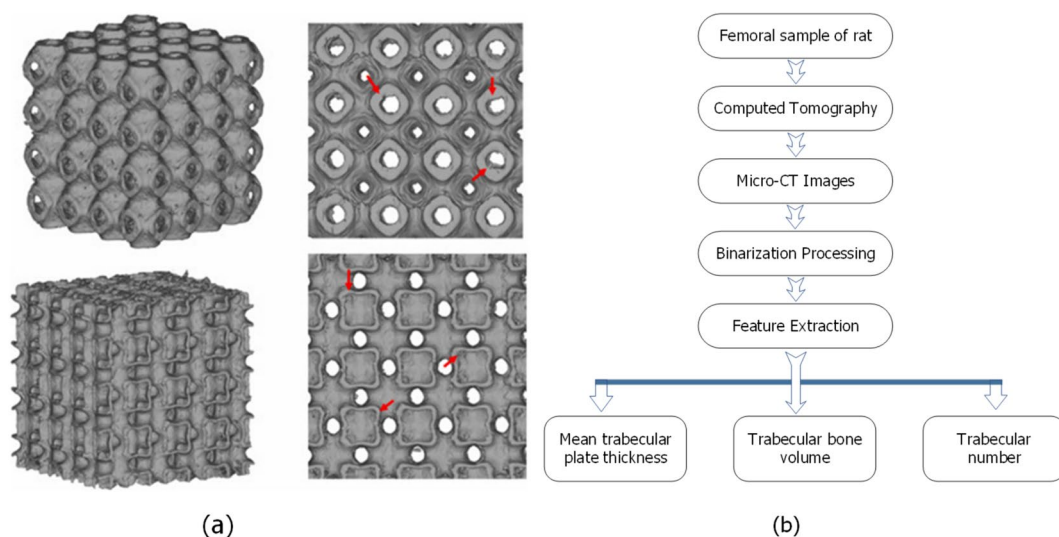

(a)   (b)

Fig. 6 **a** CT scan of printed part used to identify defects [65], **b** Flow chart illustrating the geometrical feature extraction process from a CT scan [64]

nano-topology optimization technique attempts to distribute materials at nanoscale scale through atomistic simulations that are different from classical FEM approaches that would require an excessive computational load [76].

The moving morphable component algorithm makes TO more flexible and less computationally intensive. It defines structural components any solid substance that fills a design domain volume. Therefore, an optimal structural topology can be obtained by determining the component's characteristics and by moving them in the design space [77].

In structural optimization, minimizing compliance or maximizing stiffness is the most common objective as porous structures allow for increased deformation compared to a solid one, on top of increasing the scaffold's capability for energy absorption which is important to withstand shocks [41, 63, 78]. This approach also tends to increase the metamaterial yield strength. There have been attempts to extend static compliance as an objective function into a dynamic compliance to cover vibration problems although it is a criticized approach [79, 80]. In terms of fluidic properties, the one that has been optimized the most is wall shear stress as it directly correlates with cell adhesion and differentiation [23, 25, 32, 75].

Though there exist limited studies on multi-objective optimization approaches, it is possible to combine either multiple objectives of the same nature, like stiffness under different load conditions or different quantities altogether [81, 82]. Multi-objective TO also has a heavier dependency on first guess design so testing multiple initial solutions is recommended [83]. TO can be used to create a more adequate transition region [66]. It can also be utilized to better distribute different TPMS cell types making use of their inherent characteristics where needed, leading to stiffer regions for load-bearing and porous regions for fluid transport [69], Further increase stiffness and manufacturability by optimally allocating material [16]. Also, simultaneous optimization of material distribution and unit cell topology through multi-objective approaches [68] and in design of multi-scale or hierarchical structures [84] create self-supporting structures, by introducing overhang constraints, thus reducing print times and material waste as not all TPMSs are self-supporting [42, 85]. Figure 7 showcases an example on the compliance minimizing topological optimization (TO) on a simple bending beam problem.

Based on the solution they give, algorithms are divided into two categories: gradient-based (GB) and non-gradient-based (NGB). Gradient-based algorithms make use of local searching techniques and make use of continuous variables. This causes them to be vulnerable to local minima and to output non-discrete design solutions. Both of these problems can be overcome by regularizing or convexifying the local minima and by removing the grayscale region with either a threshold value, a continuation approach or using mesh
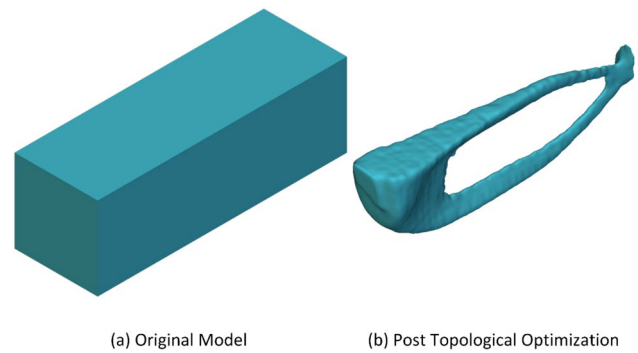

(a) Original Model   (b) Post Topological Optimization

Fig. 7 Results of a compliance minimizing TO on a simple bending beam problem **a** Original model **b** Optimized model

independent discrete solutions [86]. To counterbalance these inconveniences, GB TO is very efficient and scales linearly with mesh granularity, allowing for element numbers in the millions that are required to faithfully represent physics.

Non-gradient-based algorithms are very easy to implement and output discrete solutions. They commonly only make use of objective function values, which means that they search globally for a global optimum. Their main issue comes from their inefficient scaling with mesh quality: the exponential growth in computational cost limits their use on very coarse meshes that may be useful for initial designs but are unable to replicate physical phenomena. In order to achieve an optimized structure, the work breakdown structure starts at studying the application case since TO is heavily dependent on load cases, an accurate analysis of the forces applied on the location the scaffold will replace is very important. A first tentative CAD model is then created and meshed as a FE where a TO algorithm can be applied. It is necessary to formulate the TO problem, to describe the physics in a FEM environment, to define objectives and constraints and to define the numerical procedure used. The optimization output is another model that can be exported as an STL file that could require some post processing to become a usable CAD model. The scaffold can now undergo FEM and CFD testing to predict it's mechanical and fluidic properties. If they result satisfactory, the model can be sliced and manufactured through additive manufacturing. It is also advisable to perform either SEM or X-ray imaging on the as built part to ensure that it is acceptably similar compared to the as designed part.

4.2 Additive manufacturing technology for porous structures

Depending on materials processing technology, the American Society for Testing and Materials (ASTM) committee (ASTM F42-Additive Manufacturing) categorized Additive Manufacturing into 7 broad categories as binder jetting,

material extrusion, direct energy deposition, Vat polymerization, Sheet lamination, material jetting and powder bed fusion [87]. These technologies have become more affordable, reviving interest in intricate geometries and their potential use in engineering fields, including BTE. Several of the AM processes can be utilized to create TPMS structures, although component quality, process speed, and material availability vary greatly. The illustration of different AM technologies commonly used for the manufacturing of TPMS structures is summarized in Fig. 8.

4.2.1 Powder bed-based

4.2.1.1 Selective laser melting (SLM) and selective laser sintering (SLS) Powder bed layers are scanned by a laser spot that either melts the particles together or sinters them. In order to avoid oxidation effects at higher temperatures, it is possible to work in a protected atmosphere. As with any technology that uses powders, the size and the shape of the particles play an important role in part quality. Parts can be post-processed with sandblasting to improve surface quality, especially in cases where partially melted particles adhere to surfaces. Generally used with metallic materials and polymers [88].

Ataee et al. [89] manufactured pure titanium gyroid scaffolds making use of SLM technology, obtaining a structure with elastic modulus and yield strength similar to those of trabecular bone and with optimal ductility. The SLM process is also suited to more uncommon materials such as the Mg alloy used by Yue et al. [90] that was used to obtain both Gyroid TPMS and Voronoi-based scaffolds for comparison. SEM testing revealed that a good interconnectivity in both samples, but mechanical testing showed better mechanical performance for the TPMS-based structure. As in any manufacturing process, variability is quite important and has been studied by Lu et al. [91], in this work, 24 gyroid specimens have been printed through SLM and tested. Compressive modulus is lower than designed in both build orientations used and porosity is also lower although strain energy density resulted higher than expected. On the other hand, Li et al. [92] used SLS to print biocompatible material PA12/HA for BTE scaffold applications obtaining both graded and uniform samples of 3 non-TPMS lattice unit cells that were numerically and experimentally tested. It was observed that a different failure mode is present between graded and uniform structures as layers of different thickness present different amounts of stress. Ali Salehi et al. [93] printed primitive TPMS models with PA2200 material. 12 uniform models were tested at different cell sizes and porosity while 6 graded models were tested at different unit cell sizes with continuously
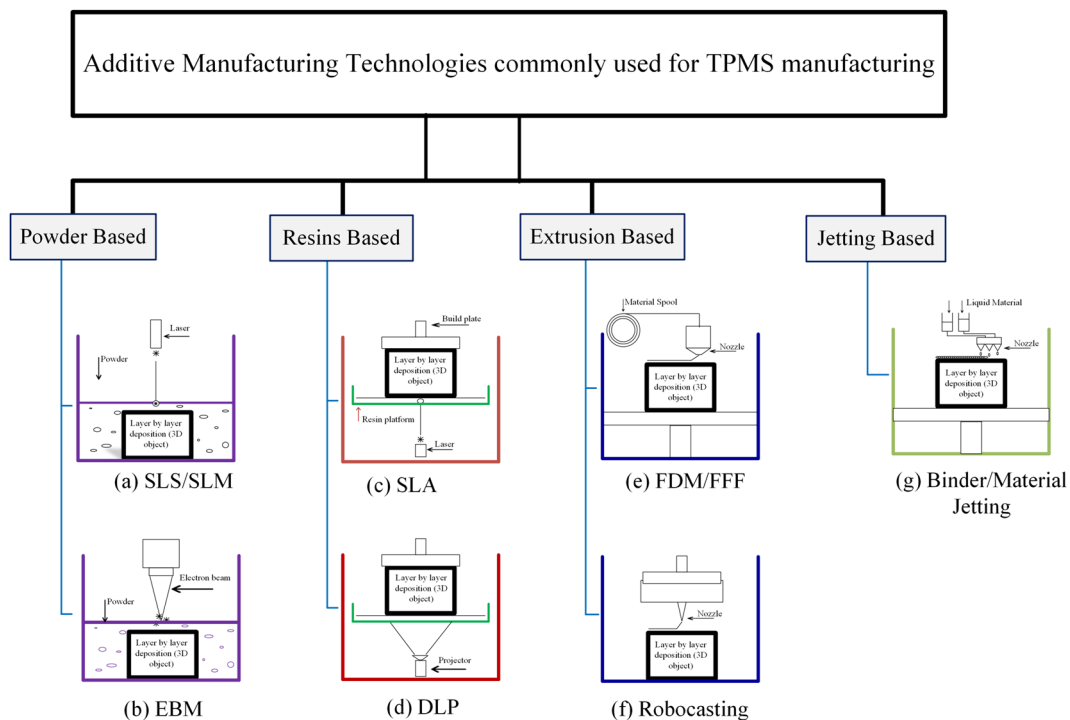

Fig. 8 Illustration of additive manufacturing processes commonly used for TPMS manufacturing. **a** Selective Laser Sintering/Selective Laser Melting **b** Electron Beam Melting **c** Stereolithography Apparatus **d** Digital Light Processing **e** Fused Deposition Modeling/Fused Filament Fabrication **f** Robocasting or Direct Ink Writing **g** Material Jetting

varying porosity or energy density, a quantity derived by process parameters.

4.2.1.2 Electron beam melting (EBM) Instead of using a laser as the heat source, this process is powered by an electron gun that heats and melts powder particles. Its spot size is generally higher than that of a laser-based system, but it is capable of reaching higher temperatures which allows to efficiently melt tough metal alloys although it is limited to conductive materials [94].

Lv et al. [95] explored biocompatibility of EBM manufactured Ti6Al4V hexagon pattern scaffolds through in vitro analysis of cytocompatibility and osteogenesis which both gave positive results suggesting suitability for medical applications. Osseointegration was also explored by Shah et al. [96] by printing Ti6Al4V and CrCo alloys samples that then got implanted for long term biocompatibility testing. Osteoblast distribution was similar in both samples showing adequate results. Table 1 summarizes the SLS and SLM AM techniques used for TPMS manufacturing.

4.2.2 Extrusion-based

4.2.2.1 Fused deposition modeling (FDM) or fused filament fabrication (FFF) Process follows layer path while depositing material from one of its nozzles. Multiple nozzles allow for use of different materials in the same build. Resolution isn't great and neither is print speed, but it is the cheapest technology available. It also requires the printing of support structures, in the case of TPMS scaffolds, it is required for those to be made of soluble materials in order to be able to remove them [97].

Mishra et al. [98] studied mechanical properties of Primitive TPMS-based lattices made of either PLA or ABS in order to observe the effect of different materials on scaffolds mechanical properties. The samples were printed through FDM technology, and these were tested at different strain rates. At higher deformation rates, strength and fracture strained were higher, except for the highest speed. As it is known, AM processes inherently introduce directionality in material properties. Aquino et al. [99] investigated the effect of load direction on FDM printed TPMS-based compression test samples showing clearly that load direction must be considered when designing TPMS-based scaffolds that are going to be manufactured through AM. Liu et al. [100] investigated cell proliferation on FFF manufactured PLA scaffolds. With less porosity, cell proliferation increased and the gyroid and diamond TPMSs performed the best.

Table 1 Summary of cited works that make use of SLS/SLM AM technologies

Technology	Material	TPMS type	Experimental tests	Numerical simulations	RD target	References
SLM	Ti6Al4V	Split P—sheet—uni Split P—skeletal—uni	Tensile Compression SEM	Compression	10.48 16.74 25.19 21 21	[28]
SLM	Ti6Al4V	Gyroid—sheet—uni Gyroid—skeletal—uni	Porosity Compression SEM	Compression Tensile	30	[50]
SLS	PA12	Primitive—sheet—uni Gyroid—sheet—uni Diamond—sheet—uni Neovius—sheet—uni	SEM Compression	Compression	10 20 30	[10]
SLM	316L stainless steel	Gyroid—sheet—uni	Compression	Compression	0.4	[44]
SLM	Commercially Pure Titanium	Gyroid—sheet—uni	X-ray Diffraction micro-CT microhardness TEM Compression	–	26.7 27.6 31.3	[89]
SLM	AZ91 Mg alloy	Hybrid Primitive-Gyroid—sheet	SEM Compression	Compression	5 8 11 14	[90]
SLS	PA2200	Primitive—skeletal—uni Primitive—skeletal—grad	Compression SEM	–	30 40 45 50 60	[93]

4.2.2.2 Robocasting or direct ink writing Makes use of pastes that retain shape when deposited. There is a higher variety of available materials, such as polymers and ceramics. The process outputs a green body that needs to undergo either sintering or curing, depending on the slurry used [101].

Baumer et al. [102] used FKS TPMS to mitigate ceramic material brittle behavior. A sample was printed through robocasting sintered and subsequently characterized, resulting in excellent morphology from the sintering process and adequate layer adhesion. Table 2 summarizes works that make use of FFF/FDM/Robocasting AM technologies.

4.2.3 Resin-based

4.2.3.1 Stereolithography apparatus (SLA) and digital light processing (DLP) The technology makes use of a dense photo-sensible resin that polymerizes when subjected to UV light provided either through a laser or a projector. The resolution is usually among the best of AM technologies but the nature of the process limits material choice to resin-like precursors to polymers or ceramic materials dispersed in a resin with a photoinitiator [104].

Zhang et al. [105] used a beta-tricalcium-based resin to build gyroid scaffolds mimicking cancellous bone. These were geometrically characterized and underwent mechanical and biocompatibility testing. The print showed no significant defects or distortions, the gyroid-based scaffold showed promising results when compared to traditional grid-like scaffolds. Whereas Shen et al. [106] created a customized material resin to use in a DLP process. TPMS-based scaffolds were manufactured and tested both for morphology,

mechanical properties, biocompatibility in vitro and lastly implanted in vivo. Although shrinkage was observed the interconnectivity was not noticeably affected. The use of bioceramics increased the expression of osteoblasts, especially for diamond and gyroid TPMSs. Similarly, Saed et al. [107] manufactured a gyroid scaffold through DLP using a custom-made resin and studied mechanical properties, porous structure, and cell viability of the structure. Also, Martìn-Montal et al. [108] investigated the effects of process parameters for SLA processes, testing for print angle, layer height and curing process. Table 3 summarizes works that make use of SLA/DLP AM technologies.

4.2.4 Jetting-based

Photopolymers are sprayed on the build surface as droplets that get immediately curated by a following UV lamp. It allows for use of different materials at the same time, including support material, that are usually hydro-soluble or with a much lower melting temperature than build materials. There is the possibility of mixing polymers to obtain composites materials with desired characteristics [109].

Summary of previous studies that make use of Multijet is presented on Table 4.

5 Discussion and future outlook

This study presents a comprehensive review of various papers to elucidate the formulation, design, and application of triply periodic minimal surfaces (TPMS), particularly in the context of bone tissue engineering scaffolds. TPMS

Table 2 Summary of works that make use of FFF/FDM/Robocasting AM technologies

Technology	Material	TPMS type	Experimental tests	Numerical Simulations	RD	Reference
FFF	PBAT-PLA composite	Gyroid—sheet—uni/graded Primitive—sheet—uni/graded	CT scan Compression Tensile	–	Same across all samples	[47]
FFF	Z-Ultrat	Neovius—skeletal—uni Gyroid—skeletal—uni Primitive—skeletal—uni Lidinoid—skeletal—uni Split P—skeletal—uni Diamond—skeletal—uni	Compression	–	Neovius—50 Split P—40 Other—30	[103]
FDM	PLA ABS	Primitive—sheet—uni	Compression SEM	–	–	[98]
FDM	ABS	Primitive—skeletal—uni Gyroid—skeletal—uni Diamond—skeletal—uni	Compression	–	30	[99]
FFF	PLA	Gyroid Diamond	Biocompatibility Compression	–	55 70 85	[100]
Robocasting	HAp+EGDMA	FKS—sheet—uni	SEM	–	26.29	[102]

Table 3 -Summary of cited works that make use of SLA/DLP AM technologies

Technology	Material	TPMS type	Experimental Tests	Numerical Sim	RD	References
SLA	UV resin	Primitive—skeletal—uni	Compression	Compression Compression-shear	–	[15]
SLA	TPGDA acrylic resin + Alumina powders	Gyroid—sheet—uni CLP—sheet—uni Primitive—sheet—uni Gyroid—skeletal—uni CLP—skeletal—uni Primitive—skeletal—uni	Compression PressureDrop SEM	Compression	29%, 25% 18%, 10% 15%, 20% 26%, 23% 20%,10% 14%, 27%	[18]
SLA	Beta-TCP	Gyroid- sheet—uni	Biocompatibility	Compression	15, 20 30, 40 50, 60	[105]
DLP	CSi-Mg6 + HDDA and TMPTA resin	Diamond—skeletal—uni Gyroid—skeletal—uni Diamond—sheet—uni Gyroid—sheet—uni IWP—skeletal—uni	SEM Compression Biodegradation Biocompatibility Implantation micro-CT	–	42	[106]
DLP	PLLA	Gyroid—sheet—uni	SEM Resin characterization Biocompatibility	–	41.3	[107]

Table 4 Summary of cited works that make use of Multijet AM technologies

Material	TPMS type	Experimental Tests	Numerical Simulations	RD	References
Visijet S300	Gyroid—sheet—uni	Micro-CT Compression	–	30% 50%	[46]
Visijet M3 crystal	Diamond—sheet—uni Gyroid—sheet—uni Primitive—sheet—uni	Permeability	Permeability	30%	[25]
Visijet M3 crystal	Diamond—sheet—uni Gyroid—sheet—uni Primitive—sheet—uni	Permeability	–	20% 30% 40% 50%	[24]
Visijet M3 crystal	Diamond—sheet—uni Gyroid—sheet—uni Primitive—sheet—uni	Compression	Compression	20% 30% 40%	[32]

structures are well-known for their inherent geometric characteristics, which allow for optimal material distribution and structural efficiency. TPMS-based structures result the superior choice when compared to strut-based alternatives as their smooth surface allows for better biomechanical properties overall. Sheet TPMS are also to be preferred compared to skeletal as thanks to their stretching deformation mode the stress distribution appears more uniform with consequent improvements over yield strength of the metamaterial and fatigue behavior.

It can be generalized that considerable progress has been achieved in the areas of optimization and additive manufacturing technologies for bone tissue engineering applications. However, a closer look at these areas reveals both encouraging possibilities and obvious shortcomings that call for more research and creativity.

The current main focus of TPMS optimization at the moment is on improving its mechanical properties and controlling porosity to fit certain applications. To optimize structural efficiency and biological compatibility, the geometrical design of TPMS has been refined through the use of advanced algorithms, including genetic algorithms, gradient-based optimization, and topological optimization. TO results a viable tool to attain ulterior improvements over TPMS structure design as it allows deeper customization options of the scaffold which allows to fine tune its behavior. Gradient-based algorithms are to be preferred over non-gradient-based ones as these are less efficient especially for dense meshes which are required to accurately simulate the physics involved. Even with these improvements, optimizing complex geometries still requires a high level of computational intensity, which frequently results in a large time and

investment in resources. On the one hand, the scalability of optimized designs, which range from small-scale models to actual applications that are bigger in scale, is another problem that continues to be experienced.

In terms of fabrication, AM results the only viable technology to create TPMS scaffolds due to their inherent complexity. These techniques enable the accurate creation of complex TPMS structures, which are essential for replicating the intrinsic porosity and mechanical characteristics of bone. Nevertheless, the resolution constraints of existing 3D printing technologies can hinder the ability to achieve the smallest possible size for TPMS pores. This is crucial for the infiltration of cells and the development of blood vessels in bone tissue engineering. Plenty of AM technologies can be utilized for this purpose although SLA is a favorite for polymers thanks to its very high resolution which results in smooth surfaces that are fundamental to cell adhesion and smooth stress distribution. In the case of metal parts, generally produced by powder-based technologies, it is recommended to post process the part to ensure adequate surface quality. Moreover, the mechanical robustness of materials utilized in 3D printing frequently falls short of that exhibited by natural bone, resulting in certain complications in load-bearing scenarios.

The functionality of 3D printed TPMS scaffolds could be improved through the development of novel bioinks that replicate the composition of natural bone extracellular matrix or incorporate growth factors. Furthermore, progressions in 3D and 4D printing technologies may facilitate the fabrication of TPMS structures that possess graded properties, thereby more closely resembling the intricate hierarchical configurations observed in natural bone.

Additionally, future research should focus on the use of fine meshes that do not employ linear tetra elements, as they are very stiff and may skew results. There is a need for the development of more TPMS modeling programs, as the available geometries are largely limited by the unit cell choice of CAD programs. The scarcity of fatigue tests and anisotropy tests in the current literature should be addressed to gain a more comprehensive understanding of TPMS scaffolds.

Declarations

Conflict of interest On behalf of all authors, the corresponding author states that there is no conflict of interest.

References

1. Kraeutler MJ, Bravman JT, McCarty EC (2013) Bone-patellar tendon-bone autograft versus allograft in outcomes of anterior cruciate ligament reconstruction: a meta-analysis of 5182 patients. Am J Sports Med 41(10):2439–2448. https://doi.org/10.1177/0363546513484127

2. Koons GL, Diba M, Mikos AG (2020) Materials design for bone-tissue engineering. Nat Rev Mater 5(8):584–603. https://doi.org/10.1038/s41578-020-0204-2

3. Donnelley CA, Shirley C, von Kaeppler EP, Hetherington A, Albright PD, Morshed S, Shearer DW (2021) Cost analyses of prosthetic devices: a systematic review. Arch Phys Med Rehabil 102(7):1404–1415. https://doi.org/10.1016/j.apmr.2021.02.010

4. Boujelbene M, Abellard P, Bayraktar E, Torbaty S (2008) Study of the milling strategy on the tool life and the surface quality for knee prostheses. J Achiev Mater Manuf Eng 31(2):610–615

5. Chatzigeorgiou C, Piotrowski B, Chemisky Y, Laheurte P, Meraghni F (2022) Numerical investigation of the effective mechanical properties and local stress distributions of TPMS-based and strut-based lattices for biomedical applications. J Mech Behav Biomed Mater 126:105025–105025. https://doi.org/10.1016/j.jmbbm.2021.105025

6. Han C, Yan C, Wen S, Xu T, Li S, Liu J, Wei Q, Shi Y (2017) Effects of the unit cell topology on the compression properties of porous Co-Cr scaffolds fabricated via selective laser melting. Rapid Prototyp J 23(1):16–27. https://doi.org/10.1108/rpj-08-2015-0114

7. Feng J, Fu J, Yao X, He Y (2022) Triply periodic minimal surface (TPMS) porous structures: from multi-scale design, precise additive manufacturing to multidisciplinary applications. Int J Extrem Manuf. https://doi.org/10.1088/2631-7990/ac5be6

8. Schwarz H (1865) De superficiebus in planum explicabilibus primorum septem ordinum. J Reine Angew Math 64:1–16. https://doi.org/10.1515/crll.1865.64.1

9. Qureshi ZA, Al-Omari SA, Burhan EE, Al-Ketan O, Al-Rub RA (2021) Using triply periodic minimal surfaces (TPMS)-based metal foams structures as skeleton for metal-foam-PCM composites for thermal energy storage and energy management applications. Int Commun Heat Mass Transf 124:105265. https://doi.org/10.1016/j.icheatmasstransfer.2021.105265

10. Kladovasilakis N, Tsongas K, Kostavelis I, Tzovaras D, Tzetzis D (2022) Effective mechanical properties of additive manufactured triply periodic minimal surfaces: experimental and finite element study. Int J Adv Manuf Technol 121(11–12):7169–7189. https://doi.org/10.1007/s00170-022-09651-w

11. Peng H, Gao F, Hu W (2019) Design, modeling and characterization on triply periodic minimal surface heat exchangers with additive manufacturing. In: 2019 international solid freeform fabrication symposium. University of Texas at Austin.

12. Yu S, Sun J, Bai J (2019) Investigation of functionally graded TPMS structures fabricated by additive manufacturing. Mater Des 182:108021. https://doi.org/10.1016/j.matdes.2019.108021

13. Triply Periodic Minimal Surfaces.; Available from: https://kenbrakke.com/evolver/examples/periodic/periodic.html

14. Minimal Surfaces. Available from: https://minimalsurfaces.blog/home/repository/triply-periodic/

15. Sengsri P, Fu H, Kaewunruen S (2022) Mechanical properties and energy-absorption capability of a 3D-printed TPMS sandwich lattice model for meta-functional composite bridge bearing applications. J Compos Sci 6(3):71. https://doi.org/10.3390/jcs6030071

16. Sharma D, Hiremath SS (2022) Additively manufactured mechanical metamaterials based on triply periodic minimal surfaces: performance, challenges, and application. Mech Adv Mater Struct 29(26):5077–5107. https://doi.org/10.1080/15376494.2021.1948151

17. Ouda M, Al-ketan O, Sreedar N, Hasan Ali MI, Abu Al-Rub RK, Hong S, Arafat HA (2020) Novel static mixers based on triply periodic minimal surface (TPMS) architectures. J Environ Chem Eng 8(5):104289. https://doi.org/10.1016/j.jece.2020.104289

18. Al-Ketan O, Pelanconi M, Ortona A, Abu Al-Rub RK (2019) Additive manufacturing of architected catalytic ceramic substrates based on triply periodic minimal surfaces. J Am Ceram 102(10):6176–6193. https://doi.org/10.1111/jace.16474

19. Lesmana LA, Aziz M (2023) Adoption of triply periodic minimal surface structure for effective metal hydride-based hydrogen storage. Energy 262:125399. https://doi.org/10.1016/j.energy.2022.125399

20. Yang W, An J, Chua CK, Zhou K (2020) Acoustic absorptions of multifunctional polymeric cellular structures based on triply periodic minimal surfaces fabricated by stereolithography. Virtual Phys Prototyp 15(2):242–249. https://doi.org/10.1080/17452759.2020.1740747

21. Martin N, Seo S, Prieto SB, Jesse C, Woolstenhulme N (2023) Reactor physics characterization of triply periodic minimal surface-based nuclear fuel lattices. Prog Nucl Energy 165:104895. https://doi.org/10.1016/j.pnucene.2023.104895

22. Song K, Wang Z, Lan J, Ma S (2021) Porous structure design and mechanical behavior analysis based on TPMS for customized root analogue implant. J Mech Behav Biomed Mater 115:104222. https://doi.org/10.1016/j.jmbbm.2020.104222

23. Ali D, Ozalp M, Blanquer SBG, Onel S (2020) Permeability and fluid flow-induced wall shear stress in bone scaffolds with TPMS and lattice architectures: a CFD analysis. Eur J Mech B Fluids 79:376–385. https://doi.org/10.1016/j.euromechflu.2019.09.015

24. Santos J, Pires T, Gouveia BP, Castro APG, Fernandes PR (2020) On the permeability of TPMS scaffolds. J Mech Behav Biomed Mater 110:103932–103932. https://doi.org/10.1016/j.jmbbm.2020.103932

25. Castro APG, Pires T, Santos JE, Gouveia BP, Fernandes PR (2019) Permeability versus design in TPMS scaffolds. Materials 12(8):1313. https://doi.org/10.3390/ma12081313

26. Dong Z, Zhao X (2021) Application of TPMS structure in bone regeneration. Eng Regen 2:154–162. https://doi.org/10.1016/j.engreg.2021.09.004

27. Mustafa NS, Akhmal NH, Izman S, Ab Talib MH, Shaiful AIM, Omar MNB, Yahaya NZ, Illias S (2021) Application of computational method in designing a unit cell of bone tissue engineering scaffold: a review. Polymers 13(10):1584. https://doi.org/10.3390/polym13101584

28. Rezapourian M, Jasiuk I, Saarna M, Hussainova I (2023) Selective laser melted Ti6Al4V split-P TPMS lattices for bone tissue engineering. Int J Mech Sci 251:108353. https://doi.org/10.1016/j.ijmecsci.2023.108353

29. Haleem A, Javaid M, Khan RH, Suman R (2020) 3D printing applications in bone tissue engineering. J Clin Orthop Trauma 11(Suppl 1):S118–S124. https://doi.org/10.1016/j.jcot.2019.12.002

30. Al-Ketan O, Lee DW, Rowshan R, Abu Al-Rub RK (2020) Functionally graded and multi-morphology sheet TPMS lattices: Design, manufacturing, and mechanical properties. J Mech Behav Biomed Mater 102:103520. https://doi.org/10.1016/j.jmbbm.2019.103520

31. Maia FR, Bastos AR, Oliveria JM, Correlo VM, Reis RL (2022) Recent approaches towards bone tissue engineering. Bone 154:116256–116256. https://doi.org/10.1016/j.bone.2021.116256

32. Castro APG, Santos J, Pires T, Fernandes PR (2020) Micromechanical behavior of TPMS scaffolds for bone tissue engineering. Macromol Mater Eng 305(12):200487. https://doi.org/10.1002/mame.202000487

33. Kang JH, Sakthiabirami K, Jang KJ, Jang JG, Oh GJ, Park C, Fisher JG, Park SW (2022) Mechanical and biological evaluation of lattice structured hydroxyapatite scaffolds produced via stereolithography additive manufacturing. Mater Des 214:110372. https://doi.org/10.1016/j.matdes.2021.110372

34. Rahmati M, Millis DK, Urbanska AM, Saeeb MR, Venugopal JR, Ramakrishna S, Mozafari M (2021) Electrospinning for tissue engineering applications. Prog mater sci 117:100721. https://doi.org/10.1016/j.pmatsci.2020.100721

35. Zhao M, Zhang DZ, Li Z, Zhang T, Zhou H, Ren Z (2022) Design, mechanical properties, and optimization of BCC lattice structures with taper struts. Compos Struct 295:115830. https://doi.org/10.1016/j.compstruct.2022.115830

36. Wei YL, Yang QS, Liu X, Tao R (2022) Multi-bionic mechanical metamaterials: a composite of FCC lattice and bone structures. Int J Mech Sci 213:106857. https://doi.org/10.1016/j.ijmecsci.2021.106857

37. Gao Y, Wei X, Han X, Zhou Z, Xiong J (2021) Novel 3D auxetic lattice structures developed based on the rotating rigid mechanism. Int J Solids Struct 233:111232. https://doi.org/10.1016/j.ijsolstr.2021.111232

38. Paul JF, Gandy, Klinowski J (2000) Exact computation of the triply periodic Schwarz P minimal surface. Chem Phys Lett 322:579–586. https://doi.org/10.1016/S0009-2614(00)00453-X

39. Pugliese R, Graziosi S (2023) Biomimetic scaffolds using triply periodic minimal surface-based porous structures for biomedical applications. SLAS Technol 28(3):165–182. https://doi.org/10.1016/j.slast.2023.04.004

40. Li L, Shi J, Zhang K, Yang L, Yu F, Zhu L, Liang H, Wang X, Jiang Q (2019) Early osteointegration evaluation of porous Ti6Al4V scaffolds designed based on triply periodic minimal surface models. J Orthop Translat 19:94–105. https://doi.org/10.1016/j.jot.2019.03.003

41. Hu C, Hu H, Lin H, Yan J (2023) Isogeometric analysis-based topological optimization for heterogeneous parametric porous structures. J Syst Sci Complex 36(1):29–52. https://doi.org/10.1007/s11424-022-1290-6

42. Zheng N, Zhai X, Chen F (2023) Topology optimization of self-supporting porous structures based on triply periodic minimal surfaces. Comput Aided Des 161:103542. https://doi.org/10.1016/j.cad.2023.103542

43. Günther F, Wagner M, Pilz S, Gebert A, Zimmermann M (2022) Design procedure for triply periodic minimal surface based biomimetic scaffolds. J Mech Behav Biomed Mater 126:104871–104871. https://doi.org/10.1016/j.jmbbm.2021.104871

44. Zhang L, Hu Z, Wang MY, Feih S (2021) Hierarchical sheet triply periodic minimal surface lattices: design, geometric and mechanical performance. Mater Des 209:109931

45. Zhao L, Jiang Z, Ma S, Zhang C, Guo W (2022) Theoretical model based on stress waves and experimental verification of residual stress in stereolithography printed ZrO$_2$ porous ceramics. Ceram Int 48(16):23983–23988. https://doi.org/10.1016/j.matdes.2021.109931

46. Castro APG, Ruben RB, Gonçalves SB, Pinheiro J, Guedes JM, Gernandes PR (2019) Numerical and experimental evaluation of TPMS Gyroid scaffolds for bone tissue engineering. Comput Methods Biomech Biomed Eng 22(6):567–573. https://doi.org/10.1080/10255842.2019.1569638

47. Cao Y, Lai S, Wu W, Sang L, Lin Y, Liu T, Liang C, Liu W, Zhao Y (2023) Design and mechanical evaluation of additively-manufactured graded TPMS lattices with biodegradable polymer composites. J Mater Res Tech 23:2868–2880. https://doi.org/10.1016/j.jmrt.2023.01.221

48. Pare A, Charbonnier B, Tournier P, Vignes C, Veziers J, Lesoeur J, Laure B, Bertin H, De Pinieux G, Cherrier G, Guicheux J, Gauthier O, Corre P, Marchat D, Weiss P (2020) Tailored three-dimensionally printed triply periodic calcium phosphate implants: a preclinical study for craniofacial bone repair. ACS Biomater Sci Eng 6(1):553–563. https://doi.org/10.1021/acsbiomaterials.9b01241

49. Carluccio D, Xu C, Venezuela J, Cao Y, Kent D, Bermingham M, Demir AG, Previtali B, Ye Q, Dargusch M (2020) Additively manufactured iron-manganese for biodegradable porous load-bearing bone scaffold applications. Acta Biomater 103:346–360. https://doi.org/10.1016/j.actbio.2019.12.018

50. Zheng X, Duan F, Song Z, Mo H, Li Z, Song Y, Su Y, Wang X (2022) A TMPS-designed personalized mandibular scaffolds with optimized SLA parameters and mechanical properties. Front Mater 9:966031. https://doi.org/10.3389/fmats.2022.966031

51. Yoo D (2013) New paradigms in hierarchical porous scaffold design for tissue engineering. Mater Sci Eng C Mater Biol Appl 33(3):1759–1772. https://doi.org/10.1016/j.msec.2012.12.092

52. Zhu LY, Li L, Li ZA, Shi JP, Tang WL, Yang JQ, Jiang Q (2019) Design and biomechanical characteristics of porous meniscal implant structures using triply periodic minimal surfaces. J Transl Med 17(1):89. https://doi.org/10.1186/s12967-019-1834-2

53. Corona-Castuera J, Rodriguez-Delgado D, Henao J, Castro-Sandoval JC, Poblano-Salas CA (2021) Design and fabrication of a customized partial hip prosthesis employing CT-scan data and lattice porous structures. ACS Omega 6(10):6902–6913. https://doi.org/10.1021/acsomega.0c06144

54. Koplin C, Schwarzer-Fischer E, Zschippang E, Löw YM, Czekalla M, Seibel A, Rörich A, Georgii J, Güttler F, Yarar-Schlickewei S, Kailer A (2023) Design of reliable remobilisation finger implants with geometry elements of a triple periodic minimal surface structure via additive manufacturing of silicon nitride. Jaaa 6(1):180–197. https://doi.org/10.3390/j6010014

55. Verma R, Kumar J, Singh NK, Rai SK, Saxena KK, Xu J (2022) Design and analysis of biomedical scaffolds using TPMS-based porous structures inspired from additive manufacturing. Coatings 12(6):839. https://doi.org/10.3390/coatings12060839

56. Germain L, Fuentes CA, van Vuure AW, des Rieux A, Dupont-Gillain C (2018) 3D-printed biodegradable gyroid scaffolds for tissue engineering applications. Mater Des 151:113–122. https://doi.org/10.1016/j.matdes.2018.04.037

57. Du X, Ronayne S, Lee SS, Hendry J, Hoxworth D, Bock R, Ferguson SJ (2023) 3D-printed PEEK/silicon nitride scaffolds with a triply periodic minimal surface structure for spinal fusion implants. ACS Appl Bio Mater 6(8):3319–3329. https://doi.org/10.1021/acsabm.3c00383

58. Qi J, Gong Y, Chen H, He J, Qiao Z, Chen Y, Shao H, Li W, Chen G, Wang M (2021) Design and 3D printing of interbody fusion cage based on TPMS porous structure. Appl Sci 11(23):11149. https://doi.org/10.3390/app112311149

59. Melchels FP, Barradas AM, van Blitterswijk CA, de Boer J, Feijen J, Grijpma DW (2010) Effects of the architecture of tissue engineering scaffolds on cell seeding and culturing. Acta Biomater 6(11):4208–4217. https://doi.org/10.1016/j.actbio.2010.06.012

60. Guerreiro R, Pires T, Guedes JM, Fernandes PR, Castro APG (2020) On the tortuosity of TPMS scaffolds for tissue engineering. Symmetry 12(4):596. https://doi.org/10.3390/sym12040596

61. Qian L, Zhang H (2011) Controlled freezing and freeze drying: a versatile route for porous and micro-/nano-structured materials. J Chem Technol Biotechnol 86(2):172–184. https://doi.org/10.1002/jctb.2495

62. Reignier J, Huneault MA (2006) Preparation of interconnected poly (ε-caprolactone) porous scaffolds by a combination of polymer and salt particulate leaching. Polymer 47(13):4703–4717. https://doi.org/10.1016/j.polymer.2006.04.029

63. Shi J, Yang J, Zhu L, Li L, Li Z, Wang X (2018) A porous scaffold design method for bone tissue engineering using triply periodic minimal surfaces. IEEE Access 6:1015–1022. https://doi.org/10.1109/ACCESS.2017.2777521

64. Karimipour-Fard P, Behravesh AH, Jones-Taggart H, Pop-Iliev R, Rizvi G (2020) Effects of design, porosity and biodegradation on mechanical and morphological properties of additive-manufactured triply periodic minimal surface scaffolds. J Mech Behav Biomed Mater 1(112):104064. https://doi.org/10.1016/j.jmbbm.2020.104064

65. AlMahri S, Santiago R, Lee DW, Ramos H, Alabdouli H, Alteneiji M, Guan Z, Cantwell W, Alves M (2021) Evaluation of the dynamic response of triply periodic minimal surfaces subjected to high strain-rate compression. Addit Manuf 46:102220. https://doi.org/10.1016/j.addma.2021.102220

66. Zhang S, Da D, Wang Y (2022) TPMS-infill MMC-based topology optimization considering overlapped component property. Int J Mech Sci 235:107713. https://doi.org/10.1016/j.ijmecsci.2022.107713

67. El Khadiri I, Abouelmajd M, Zemzami M, Hmina N, Lagache M, Al Mangour B Bahlaoui A, Arroub I, Belhouideg S (2022) TPMS lattice structure derived using topology optimization for the design of additive manufactured components. In: 2022 8th international conference on optimization and applications (ICOA). IEEE. https://doi.org/10.1109/ICOA55659.2022.9934649

68. Modrek M, Viswanath A, Khan KA, Ali MIH, Al-Rub RKA (2023) Multi-objective topology optimization of passive heat sinks including self-weight based on triply periodic minimal surface lattices. Stud Therm Eng 42:102684. https://doi.org/10.1016/j.csite.2022.102684

69. Feng Y, Huang T, Gong Y, Jia P (2022) Stiffness optimization design for TPMS architected cellular materials. Mater Des 222:111078. https://doi.org/10.1016/j.matdes.2022.111078

70. Viswanath A, Modrek M, Khan K A, Al-Rub R K A (2021) Deep learning for topology optimization of triply periodic minimal surface based gyroid-like structures. In: Proceedings of the American society for composites–thirty-sixth technical conference on composite materials. https://doi.org/10.12783/asc36/35824

71. Alkebsi EAA, Ameddah H, Outtas T, Almutawakel A (2021) Design of graded lattice structures in turbine blades using topology optimization. Int J Comput Integr Manuf 34(4):370–384. https://doi.org/10.1080/0951192X.2021.1872106

72. Pires THV, Dunlop JWC, Castro APG, Fernandes PR (2022) Wall shear stress analysis and optimization in tissue engineering TPMS scaffolds. Materials 15(20):7375. https://doi.org/10.3390/ma15207375

73. Dhingra AK, Bennage WA (1995) Topological optimization of truss structures using simulated annealing. Eng Optim 24(4):239–259. https://doi.org/10.1080/03052159508941192

74. Huang X, Xie YM (2010) A further review of ESO type methods for topology optimization. Struct Multidiscip Optim 41(5):671–683. https://doi.org/10.1007/s00158-010-0487-9

75. Van Dijk NP, Maute K, Langelaar M, van Keulen F (2013) Level-set methods for structural topology optimization: a review. Struct Multidiscip Optim 48(3):437–472. https://doi.org/10.1007/s00158-013-0912-y

76. Chen CT, Chrzan DC, Gu GX (2020) Nano-topology optimization for materials design with atom-by-atom control. Nat Commun 11(1):3745. https://doi.org/10.1038/s41467-020-17570-1

77. Zhang W, Yuang J, Zhang J, Guo X (2015) A new topology optimization approach based on Moving Morphable Components (MMC) and the ersatz material model. Struct Multidiscip Optim 53(6):1243–1260. https://doi.org/10.1007/s00158-015-1372-3

78. Strömberg N (2022) A new multi-scale topology optimization framework for optimal combinations of macro-layouts and local gradings of TPMS-based lattice structures. Mech Based Des Struct Mach 52(1):257–274. https://doi.org/10.1080/15397734.2022.2107538

79. Ma ZD, Kikuchi N, Higawara I (1993) Structural topology and shape optimization for a frequency response problem. Comput Mech 13:157–174. https://doi.org/10.1007/BF00370133

80. Silva OM, Neves MM, Lenzi A (2019) A critical analysis of using the dynamic compliance as objective function in topology optimization of one-material structures considering steady-state forced vibration problems. J Sound Vib 444:1–20. https://doi.org/10.1016/j.jsv.2018.12.030

81. Behrou R, Pizzolato A, Forner-Cuenca A (2019) Topology optimization as a powerful tool to design advanced PEMFCs flow fields. Int J Heat Mass Transf 135:72–92. https://doi.org/10.1016/j.ijheatmasstransfer.2019.01.050

82. Iqbal T, Wang L, Li D, Dong E, Fan H, Fu J, Hu C (2019) A general multi-objective topology optimization methodology developed for customized design of pelvic prostheses. Med Eng Phys 69:8–16. https://doi.org/10.1016/j.medengphy.2019.06.008

83. Li H, Ding X, Meng F, Jing D, Xiong M (2019) Optimal design and thermal modelling for liquid-cooled heat sink based on multi-objective topology optimization: an experimental and numerical study. Int J Heat Mass Transf 144:118638. https://doi.org/10.1016/j.ijheatmasstransfer.2019.118638

84. Jihong Z, Han Z, Chuang W, Lu Z, Shangqin Y, Zhang W (2021) A review of topology optimization for additive manufacturing: Status and challenges. Chin J Aeronaut 34(1):91–110. https://doi.org/10.1016/j.cja.2020.09.020

85. Liu J, Gaynor AT, Chen S, Kang Z, Suresh K, Takezawa A, Li L, Kato J, Tang J, Wang CCL (2018) Current and future trends in topology optimization for additive manufacturing. Struct Multidiscipl Optim 57(6):2457–2483. https://doi.org/10.1007/s00158-018-1994-3

86. Sigmund O (2011) On the usefulness of non-gradient approaches in topology optimization. Struct Multidiscipl Optim 43:589–596. https://doi.org/10.1007/s00158-011-0638-7

87. Adugna YW, Akessa AD, Lemu HG (2021) Overview study on challenges of additive manufacturing for a healthcare application. IOP Conf Ser Mater Sci Eng 1201(1):012041. https://doi.org/10.1088/1757-899X/1201/1/012041

88. Brighenti R, Cosma MP, Marsavina L, Spagnoli A, Terzano M (2021) Laser-based additively manufactured polymers: a review on processes and mechanical models. J Mater Sci 56:961–998. https://doi.org/10.1007/s10853-020-05254-6

89. Ataee A, Li Y, Brandt M, Wen C (2018) Ultrahigh-strength titanium gyroid scaffolds manufactured by selective laser melting (SLM) for bone implant applications. Acta Mater 158:354–368. https://doi.org/10.1016/j.actamat.2018.08.005

90. Yue X, Shang J, Zhang M, Hur B, Ma X (2022) Additive manufacturing of high porosity magnesium scaffolds with lattice structure and random structure. Mater Sci Eng A 859:144167. https://doi.org/10.1016/j.msea.2022.144167

91. Lu Y, Cui Z, Cheng L, Li J, Yang Z, Zhu H, Wu C (2020) Quantifying the discrepancies in the geometric and mechanical properties of the theoretically designed and additively manufactured scaffolds. J Mech Behav Biomed Mater 112:104080. https://doi.org/10.1016/j.jmbbm.2020.104080

92. Li J, Zhao Z, Yan R, Yang Y (2020) Mechanical properties of graded scaffolds developed by curve interference coupled with selective laser sintering. Mater Sci Eng C Mater Biol Appl 116:111181. https://doi.org/10.1016/j.msec.2020.111181

93. Salehi A, Daneshmehr A, Aminfar K (2022) Mechanical properties of materially and geometrically gradient cellular structures manufactured with SLS 3D printer applicable as a bone implant. Int J Adv Des Manuf Technol 15(1):143–155. https://doi.org/10.30495/admt.2022.1930119.1283

94. Kolamroudi M, Asmael M, Ilkan M, Kordani N (2021) Developments on electron beam melting (EBM) of Ti–6Al–4V: a review. Trans Indian Inst Met 74:783–790. https://doi.org/10.1007/s12666-021-02230-9

95. Lv J, Jia Z, Li J, Wang Y, Yang J, Xiu P, Zhang K, Cai H, Liu Z (2015) Electron beam melting fabrication of porous Ti6Al4V scaffolds: cytocompatibility and osteogenesis. Adv Eng Mater 17(9):1391–1398. https://doi.org/10.1002/adem.201400508

96. Shah FA, Omar O, Suska F, Snis A, Matic A, Emanuelsson L, Norlindh B, Lausmaa J, Thomsen P, Palmquist A (2016) Long-term osseointegration of 3D printed CoCr constructs with an interconnected open-pore architecture prepared by electron beam melting. Acta Biomater 36:296–309. https://doi.org/10.1016/j.actbio.2016.03.033

97. Kristiawan R, Imaduddin F, Ariawan D, Ubaidillah, Arifin Z (2021) A review on the fused deposition modeling (FDM) 3D printing: filament processing, materials, and printing parameters. Open Eng 11(1):639–649. https://doi.org/10.1515/eng-2021-0063

98. Mishra AK, Chavan H, Kumar A (2021) Effect of material variation on the uniaxial compression behavior of FDM manufactured polymeric TPMS lattice materials. Mater Today Proc 46:7752–7759. https://doi.org/10.1016/j.matpr.2021.02.276

99. Aquino DA, Maskery I, Longhitano GA, Jardini AL, del Conte EG (2020) Investigation of load direction on the compressive strength of additively manufactured triply periodic minimal surface scaffolds. Int J Adv Manuf Technol 109(3–4):771–779. https://doi.org/10.1007/s00170-020-05706-y

100. Liu Q, Wei F, Coathup M, Shen W, Wu D (2023) Effect of porosity and pore shape on the mechanical and biological properties of additively manufactured bone scaffolds. Adv Healthc Mater 12(30):2301111. https://doi.org/10.1002/adhm.20230 1111

101. Paterlini A, Le Grill S, Brouillet F, Combes C, Grossin D, Bertrand G (2021) Robocasting of self-setting bioceramics: from paste formulation to 3D part characteristics. Open Ceram 5:100070. https://doi.org/10.1016/j.oceram.2021.100070

102. Baumer V, Gunn E, Riegle V, Bailey C, Shonkwiler C, Prawel D (2023) Robocasting of ceramic fischer-koch s scaffolds for bone tissue engineering. J Funct Biomater. https://doi.org/10.3390/jfb14050251

103. Miralbes R, Ranz D, Pascual FJ, Zouzias D, Maza M (2022) Characterization of additively manufactured triply periodic minimal surface structures under compressive loading. Adv Mater Struct 29(13):1841–1855. https://doi.org/10.1080/15376494.2020.1842948

104. Huang J, Qin Q, Wang J (2020) A review of stereolithography: Processes and systems. Processes 8(9):1138. https://doi.org/10.3390/pr8091138

105. Zhang Y, Zhang Q, He F, Zuo F, Shu X (2022) Fabrication of cancellous-bone-mimicking β-tricalcium phosphate bioceramic scaffolds with tunable architecture and mechanical strength by stereolithography 3D printing. J Eur Ceram Soc 42(14):6713–6720. https://doi.org/10.1016/j.jeurceramsoc.2022.07.033

106. Shen M, Li Y, Lu F, Gou Y, Zhong C, He S, Zhao C, Yang G, Zhang L, Yang X, Gou Z, Xu S (2023) Bioceramic scaffolds with triply periodic minimal surface architectures guide early-stage bone regeneration. Bioact Mater 25:374–386. https://doi.org/10.1016/j.bioactmat.2023.02.012

107. Saed M, Arvin BB, Amir HH, Sadegh A, Seyyed AAA, Benham P (2020) Functionalized poly l-lactic acid synthesis and optimization of process parameters for 3D printing of porous scaffolds via digital light processing (DLP) method. J Manuf Process 56:550–561. https://doi.org/10.1016/j.jmapro.2020.04.076

108. Martin-Montal J, Pernas-Sanchez J, Varas D (2021) Experimental characterization framework for SLA additive manufacturing materials. Polymers 13(7):1147. https://doi.org/10.3390/polym13071147

109. Gülcan O, Günaydın K, Tamer A (2021) The state of the art of material jetting—a critical review. Polymers 13(16):2829. https://doi.org/10.3390/polym13162829

Publisher's Note Springer Nature remains neutral with regard to jurisdictional claims in published maps and institutional affiliations.